N65-88852
~~X63 15781~~
Code 2A
(NASA TMX 50738)

19p.

MEASURED VARIATIONS IN THE TRANSFER FUNCTION OF A HUMAN PILOT

James J. Adams and Hugh P. Bergeron

3 refs

NASA Langley Research Center
Langley Station, Hampton, Va.

Presented at the AIAA-ASD Vehicle Design and Propulsion Meeting

Dayton, Ohio
November 4-6, 1963

~~Available to NASA Offices and~~
~~NASA Centers Only~~

MEASURED VARIATIONS IN THE TRANSFER FUNCTION OF A HUMAN PILOT

James J. Adams
Aerospace Engineer
NASA Langley Research Center

Hugh P. Bergeron
Aerospace Engineer
NASA Langley Research Center

15781

Abstract

A method for determining the transfer function of a human pilot as he operates on a closed-loop control system has been devised and used in single-axis compensatory tracking tasks, and two-axis tasks both with and without cockpit movement. The transfer functions were then used to analytically obtain closed-loop characteristics.

Available to NASA Offices and NASA Centers Only.

MEASURED VARIATIONS IN THE TRANSFER FUNCTION OF A HUMAN PILOT

James J. Adams
Aerospace Engineer
NASA Langley Research Center

Hugh P. Bergeron
Aerospace Engineer
NASA Langley Research Center

Introduction

In recent years many investigations have been directed toward obtaining quantitative measures of how a pilot operates in a closed-loop tracking task. The methods used have suffered from the undesirable feature of requiring several lengthy and complicated computational steps to arrive at an answer in the desired form of a transfer function. A transfer function answer is desirable because it describes several related parameters in a concise and familiar form, and it can be used in further analytical studies of complete systems. Therefore, a method for automatically determining the transfer function of a human as he operates in a closed-loop control situation has been devised and used. The method gives continuous and instantaneous records of the gains in an analog model of the pilot.

Methods

The form of the analog model is preselected and does not vary during a given experiment. The model is mechanized by the use of an analog computer, and the computation needed to adjust the gains in the model automatically are also performed by the computer. A block diagram of the tests is shown in figure 1. The control loop for the initial tests consisted of an oscilloscope display, a lightweight spring-restrained center-located control stick, simulated dynamics, and a random disturbance signal which was summed with the output of the dynamics. The resulting error was displayed to create a compensatory tracking task. The input signal to the pilot was also introduced into the analog pilot and the output of the pilot and analog pilot are compared. The analytical form of the analog pilot, as given in figure 1, contains three variable gains; a static gain K_1, a lead gain K_2, and two equal lags τ. The assumption of this form of transfer function implies that the pilot uses the sum of the displayed error, with a gain of K_1, and the rate of change of error, with a gain of K_2, to command his controller output. This command signal is expressed by the numerator of the transfer function. It is further assumed that this command signal is applied with some lag, which is expressed by the denominator of the transfer function. Inclusion of a second-order lag is necessary to account for the inertia of the controller. For the present investigation this second-order lag was initially assumed to be expressed as two equal first-order lag terms. The use of other arrangements of the expression for lag will be discussed later. The gains K_1, K_2, and τ are adjusted by setting the rate of change of the particular gain under consideration equal to the product of the difference between the pilot and analog pilot and a weighting function obtained from the block labeled filter. Such an adjustment loop is provided for each gain to be varied, and all are adjusted simultaneously.

The type of parameter tracking just described is similar to other methods which have been proposed,[1,2] and a comparison of this method with two other methods is given in figure 2. The common feature of the three methods is that the rate of change of the adjustable gains is made proportional to the product of an error and a partial derivative of the error with respect to the gain being considered. In general, the model can be expressed as a polynomial, which for the present explanation will be expressed as a numerator and denominator. The equation error method uses an error obtained as shown (output multiplied by the denominator minus input multiplied by the numerator) times the partial which will in general be a function of the input multiplied by a function of the model form and the output multiplied by a function of the model form. In the output error method, the error is obtained as the difference between the model and the pilot, and the partial is the same as for the equation error method. In the present method the error used is the same as that used in the output error method, but by manipulation of the various signals in the model, the input and output quantities in the partial are replaced by the signal to the gain being considered. For the model being used in the present investigation, this manipulation results in simpler partial expressions.

Single-Axis Tests

The method described above has been used to measure the best fitting linear transfer function for several NASA test pilots. The first tests involved single-degree-of-freedom fixed-base simulation of dynamics that varied from an easy-to-handle rate mechanism, $2/s$, to more difficult acceleration mechanism, $10/s^2$. The purpose of the investigation was to determine the variation in the control technique used by the pilots with the various controlled elements.

Time histories of a typical test are shown in figure 3. Shown are the disturbances used, the displayed error, the pilot's output, the analog pilot's output, and the difference between the pilot and analog pilot. It can be seen that the analog pilot accurately reproduces the overall characteristics of the pilot, mainly lacking the high-frequency components of the pilot's output. The adjustment of the gains in the analog pilot is shown in figure 4. The required initial adjustment is completed in approximately 5 seconds in this case, and the variations in the gains that occur after this initial adjustment are quite small. The amplitude of these small variations increased as the difficulty of the dynamics increased, that is, the measured gains were most steady with dynamics of $2/s$, and least so for $10/s^2$. The difference between the pilot and analog pilot also increased with increase in the difficulty of the dynamics.

A listing of results obtained with the various dynamics tested for one of the subjects is shown in figure 5. The dynamics are listed in a very logical order. The first, $2/s$, is a pure rate dynamics and simulates a mechanism in which the rate of change of attitude is always exactly proportional to stick deflection. It is not possible to achieve this type of response in a vehicle which has inertia. The next two listings, $\frac{10}{s(s + 2.5)}$ and $\frac{10}{s(s + 1)}$, are also called rate systems, but now there is a lag present in the development of the rate output. These dynamics are representative of the roll mode of motion of an airplane, or of a spacecraft with linear damping augmentation. The fourth, $10/s^2$, contains an infinite amount of lag in the buildup of rate and is therefore distinguished with the name of acceleration dynamics to indicate that the acceleration of the vehicle is proportional to stick deflection. The order of these four dynamics corresponds to the amount of lag, or the amount of damping, present in the dynamics. The last dynamics listed, $\frac{10}{s(s^2 + 3s + 10)}$, is representative of airplane pitch mode of motion, and although it is the highest order system listed, it is easier to handle than some of the others.

The measured pilot transfer function coefficients obtained with the various dynamics are listed in figure 5. A very noticeable feature of the results is the way in which the measured lag coefficient, τ, increases with increase in the lag of the dynamics. These measurements lead to the logical conclusion that the lag of the pilot decreases with an increase in the lag of the vehicle which he is controlling.

The determination of the pilot's transfer function coefficients still does not allow a quantitative judgment to be made. However, once these measurements have been made, it is possible to use them in the calculation of the closed-loop characteristics of the complete system of pilot plus dynamics. Such calculated characteristics are also listed in figure 5. Now servomechanism experience can be used to make a quantitative judgment of these systems. Servomechanism theory indicates that the frequency of a system should be as high as possible, the damping ratio should ideally be 0.7, and any real roots should be negative and as high as possible. Using the damping ratio criterion, the data show that a nearly ideal system is obtained with the rate dynamics, $2/s$, and the rest of the data give a quantitative measure of how large a deviation from ideal is obtained with the other dynamics. It can be seen that the damping ratio of the complete system decreases as the lag of the dynamics increases. This same trend was found with all of the subjects tested.

The performance factor, root-mean-square error, was also measured in these tests, and these results are presented in figure 5. The values obtained confirm the fact that the acceleration dynamics were the most difficult to control. The trend in the root-mean-square error values with dynamics is what would be expected on the basis of the calculated system characteristics and, therefore, also confirms the calculated data.

Tests and measurements such as made in this part of the investigation can give quantitative indications of what changes in system characteristics will occur when any element in the control loop is changed. For example, a brief study was made of the effect that changing display sensitivity will have. These tests were done with $\frac{10}{s(s + 1)}$ dynamics, and with constant stick sensitivity. The results, presented in figure 6, show that as the display sensitivity is changed so that the indicator moves less and less, the frequency of the oscillatory characteristic decreases and the damping ratio increases. The method can be used in any particular case to determine the change in system characteristics that results from a change in some element of the control system.

Two-Axes Tests

Tests have also been made of a two-axis task, both with and without motion. The two axes were the pitch and roll axes, the display was an 8-ball instrument, and control was exercised with a two-axis side-arm controller. The simulated dynamics were $\frac{K}{s(s + 1)}$. These tests were made in a gimbal-mounted cockpit, and were conducted with the gimbals fixed and only the instrument moving, and with both the instrument and cockpit gimbals moving in a manner described by the error time history. The pitch and roll axes were analyzed separately. Roll-axis results without motion are presented in figure 7. The main feature of these results, as compared with the single-axis tests, is the variation with time in the measured gains. It can be seen that the lead gain, K_2, varies from 0 to 10, and that there are brief periods when K_1 is reduced to approximately 50 percent of its steady value. The addition of motion to the tests greatly reduced the unsteadiness in the measured gains as is shown in figure 8. These results indicate that the addition of motion cues is a help to the pilot in maintaining the quality of his control.

Comparison of Pilot and Model

Pilot Performance

The validity of the matching technique can be evaluated by noting the similarity between the output of analog pilot and the pilot. In all of the tests performed so far the analog pilot has reproduced the obvious features of the control of all the various subjects in all of the various control loops tested. That is, the analog pilot displays wave shapes and amplitudes similar to the pilot. As a further check, the measured analog pilot has been inserted into the control loop in place of the pilot, and a comparison has been made between the control error obtained with the pilot and with the analog pilot. Figure 9 shows time histories obtained in this manner in which the single-degree-of-freedom tests with the $2/s$ controlled dynamics were used. The figure presents the disturbance, the error, and the stick output that occurred with the pilot in the loop, and the error and control output with the analog pilot in the loop. It can be seen that the results obtained with the pilot and analog pilot are remarkably similar. However, when the same calculations are made using the $\frac{10}{s(s + 1)}$ dynamics, it can

be seen (fig. 10) that the use of the analog pilot results in better control than obtained with the pilot. In instances when a sharp disturbance occurs, the response with the pilot and analog pilot are very similar, but during periods when the disturbance is very mild, larger errors occur with the pilot controlling than with the analog pilot. The root-mean-square error with the pilot controlling was 1.6 volts, and with the analog pilot the root-mean-square error is 0.86 volt. These results indicate that those control motions made by the pilot that do not correlate with the linear model output are not useful. The reasons and implications of this result should be given further study.

Effect of Change in Model Form

It was stated at the beginning that the form of the model was not changed in these tests, only the gains contained in the model were varied to achieve the desired fit of the model to the pilot. For the purpose of determining whether changing the form of the analog pilot would result in a better fit, several variations in the form were tried. The two linear terms in the denominator, which were made to be identical in the original form, were allowed to adjust independently in one case, whereas a second form in which the denominator was arranged as a quadratic instead of two linear terms was tried in another case. Each of the three forms was also tried with a fixed time delay included. Several different values of the fixed delay were tried. Example time histories of analog pilot output obtained with the different forms using the same tape recorded data with the $\frac{10}{s(s + 1)}$ dynamics are shown in figure 11. The time delay used in two plots that include time delay is 0.15 second. Longer delays than this caused a noticeable deterioration in the fit of the model time history to the pilot. Although the results are slightly different with each form, there is no clear advantage of one form over another. A summary of the numerical values of the gains obtained with the different forms with the $\frac{10}{s(s + 1)}$ dynamics is presented in figure 12. The closed-loop characteristic obtained with the linear forms (those without time delays) are also presented. It can be seen that although the measured gains varied with the different forms, the closed-loop characteristics were very nearly the same in each case. The same general remarks as given here for the $\frac{10}{s(s + 1)}$ dynamics applied to all the dynamics tested. The addition of the time delay caused an increase in the lag coefficient. Although an improvement in the fit was not obtained with either of the alternate forms tried, the additional tests did provide an independent check on the closed-loop characteristics obtained with the original measurements.

Tests such as those described herein will be continued to obtain information on two- and three-axes tasks. Also, further tests which will include linear saturated and on-off control forces will be made.

References

1. Ornstein, George N.: Application of a Technique for the Automatic Analog Determination of Human Response Equation Parameters. Rep. No. NA61 H-1, North American Aviation, Inc., Jan. 2, 1961.

2. Wertz, H. J.: A Learning Model to Evaluate and Aid Human Operator Adaptation. Presented at International Congress on Human Factors in Electronics (Long Beach, Calif.), IRE, May 3-4, 1962.

3. Adams, James J., and Bergeron, Hugh P.: Measured Variations in the Transfer Function of a Human Pilot in Single-Axis Tasks. NASA TN D-1952, 1963.

Biography

James J. Adams. Born June 14, 1926 in Mitchell, South Dakota. Attended elementary school in Rocky Mount, North Carolina. Received a Bachelor of Mechanical Engineer degree from North Carolina State College in 1948. Started work with NACA in 1948 in Flight Research Division where he worked on aircraft handling-qualities measurements, and analytical studies of automatic control system to improve the gust response of aircraft and to permit blind landing. At present he is project engineer in Space Mechanics Division of NASA where he has worked on automatic altitude control systems for satellites, and on the measurement of human transfer functions.

Hugh P. Bergeron. Born May 22, 1936 in Eunice, Louisiana. Attended the University of Southwestern Louisiana and received a Bachelor degree in Physics in 1962. Started work with NASA in 1962 in Space Mechanics Division and became engaged in work on human transfer functions.

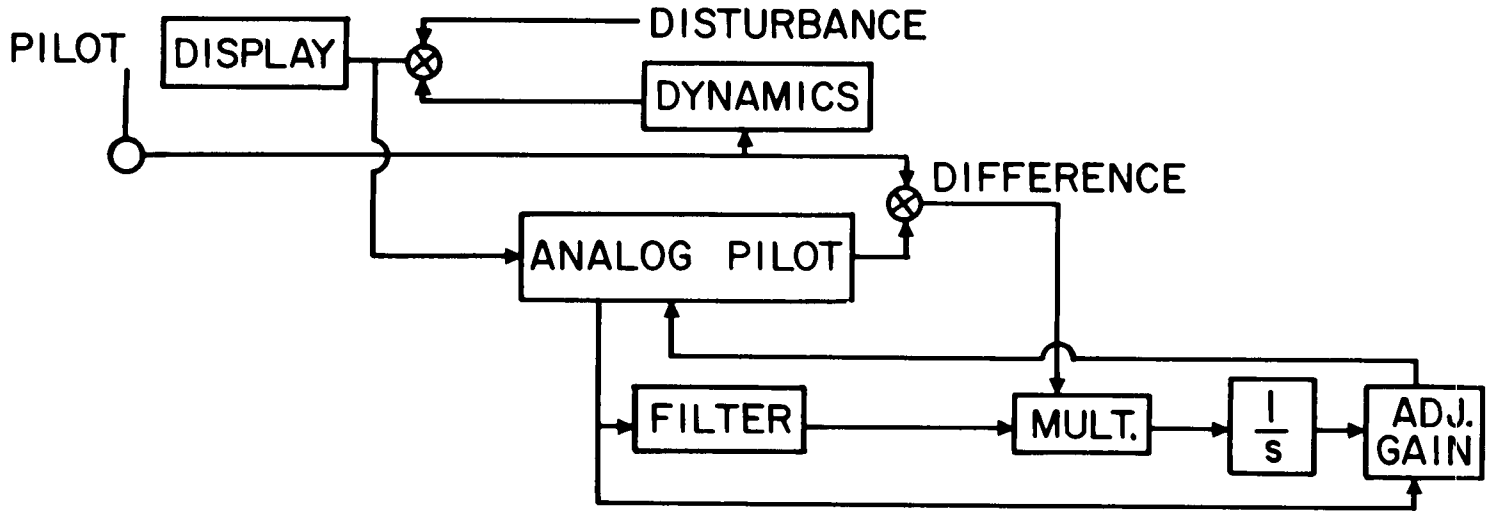

$$\frac{\text{ANALOG-PILOT OUTPUT}}{\text{INPUT}} = \frac{K_1 \tau \left(1 + \frac{K_2}{\tau} s\right)}{(\tau + s)^2}$$

NASA

Figure 1.- Block diagram of test equipment.

MODEL FORM, $\frac{\theta}{I} = \frac{N(s)}{D(s)}$

$$\dot{\alpha} = Ke\frac{\partial e}{\partial \alpha}$$

EQUATION ERROR METHOD, REFERENCE 1

$$\dot{\alpha} = K\left[\theta(D(s)) - I(N(s))\right]\left[I\left(f\frac{N(s)}{D(s)}\right), \theta\left(f\frac{N(s)}{D(s)}\right)\right]$$

OUTPUT ERROR METHOD, REFERENCE 2

$$\dot{\alpha} = K\left[I\frac{N(s)}{D(s)} - \theta p\right]\left[I\left(f\frac{N(s)}{D(s)}\right), \theta\left(f\frac{N(s)}{D(s)}\right)\right]$$

PRESENT METHOD, REFERENCE 3

$$\dot{\alpha} = K\left[I\frac{N(s)}{D(s)} - \theta p\right]\left[\delta\left(f\frac{N(s)}{D(s)}\right)\right]$$

WHERE δ = SIGNAL TO GAIN α

NASA

Figure 2.- Comparison of parameter tracking methods.

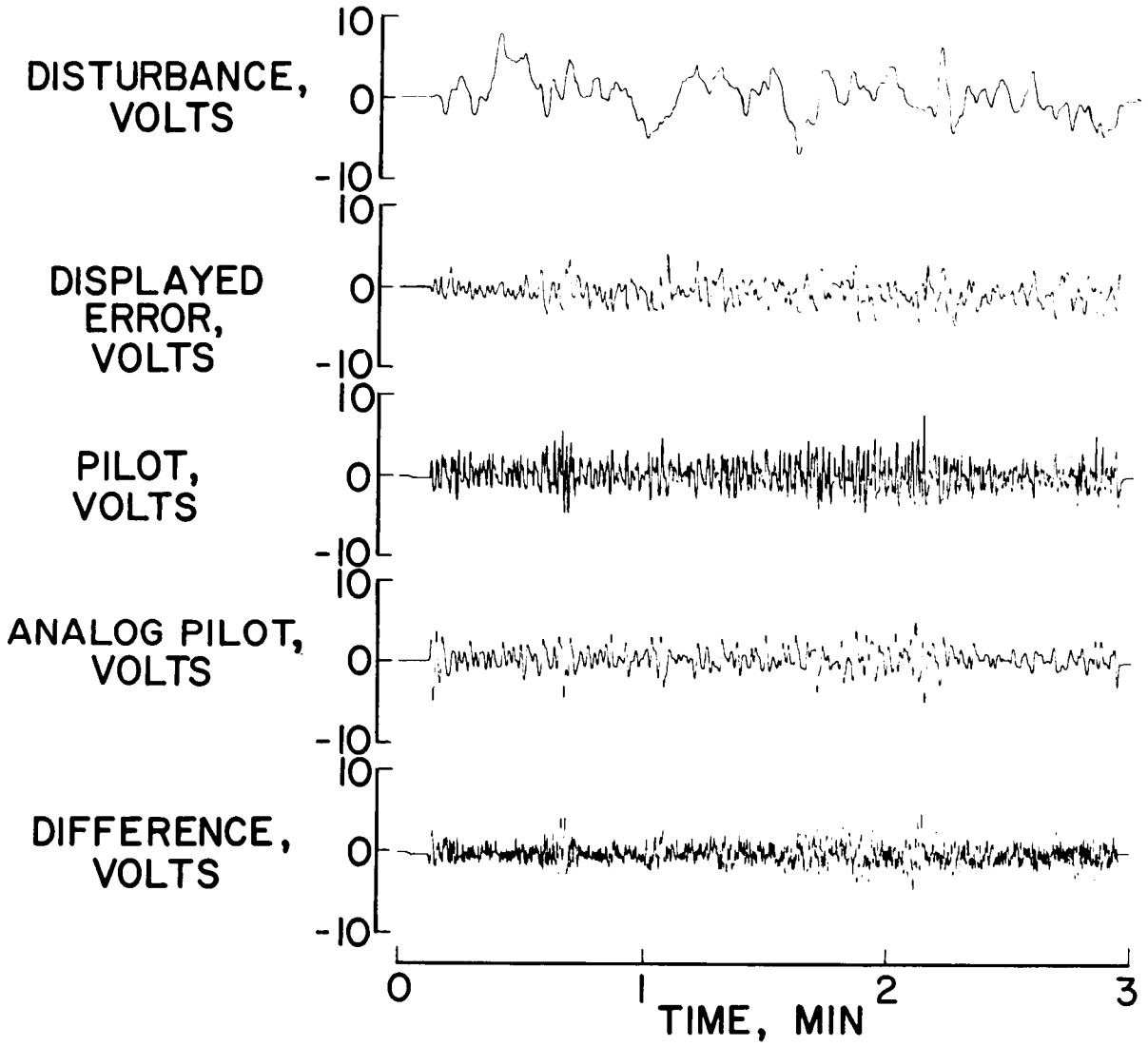

NASA

Figure 3.- Sample run with a dynamics of $\frac{10}{s(s+1)}$.

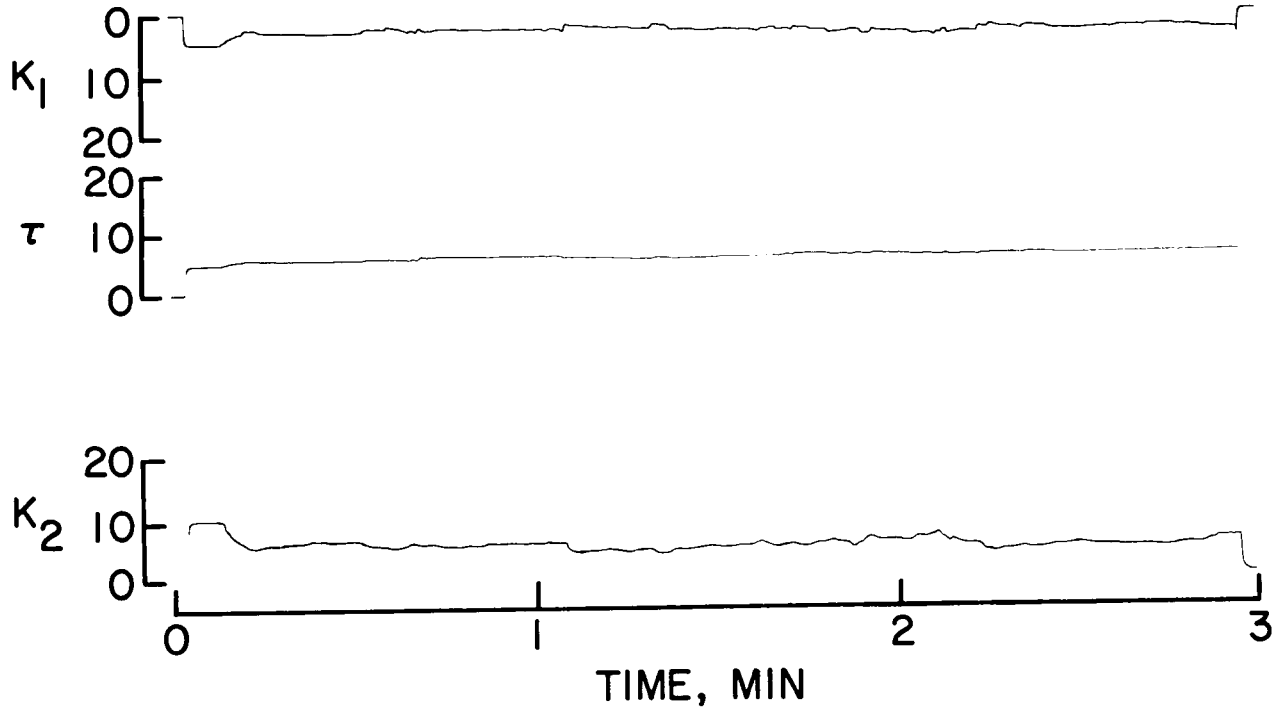

NASA

Figure 4.- Measured gains with a dynamics of $\frac{10}{s(s+1)}$.

DYNAMICS	MEASURED GAINS			CLOSED-LOOP CHARACTERISTICS			RMS ERROR, VOLTS
				OSCILLATORY		REAL ROOTS	
	K_1	τ	K_2	ω, RADIANS/SEC	ζ		
$2/s$	4	3	2	4.36	0.54	-1.26	0.7
$\frac{10}{s(s+2.5)}$	3	5	2	2.8	0.40	-2.5, -7.78	1.2
$\frac{10}{s(s+1)}$	2.5	6.5	5.5	3.45	0.37	-1.24, -10.1	1.6
$\frac{10}{s^2}$	3	7	6.5	3.71	0.21	-1.38, -10.9	2.2
$\frac{10}{s(s^2+3s+10)}$	6	7	5	3.20 7.9	0.18 0.96	-0.6	1.6

UNCONTROLLED RMS ERROR = 2.7 VOLTS

NASA

Figure 5.- Summary of single-axis test.

DISPLAY SENSITIVITY	MEASURED GAINS			CLOSED LOOP CHARACTERISTICS		
				OSCILLATORY		REAL ROOTS
	K_1	τ	K_2	ω, RADIANS/SEC	ζ	
1.25 VOLTS/INCH	5.5	8	5.5	4.66	0.28	-1.58, -12.7
5.00 VOLTS/INCH	2.2	6.5	5.5	3.46	0.37	-1.24, -10.1
50.00 VOLTS/INCH	1	6	5	2.17	0.70	-1.51, -8.41

NASA

Figure 6.- Effect of display sensitivity with a dynamics of $\frac{10}{s(s + 1)}$.

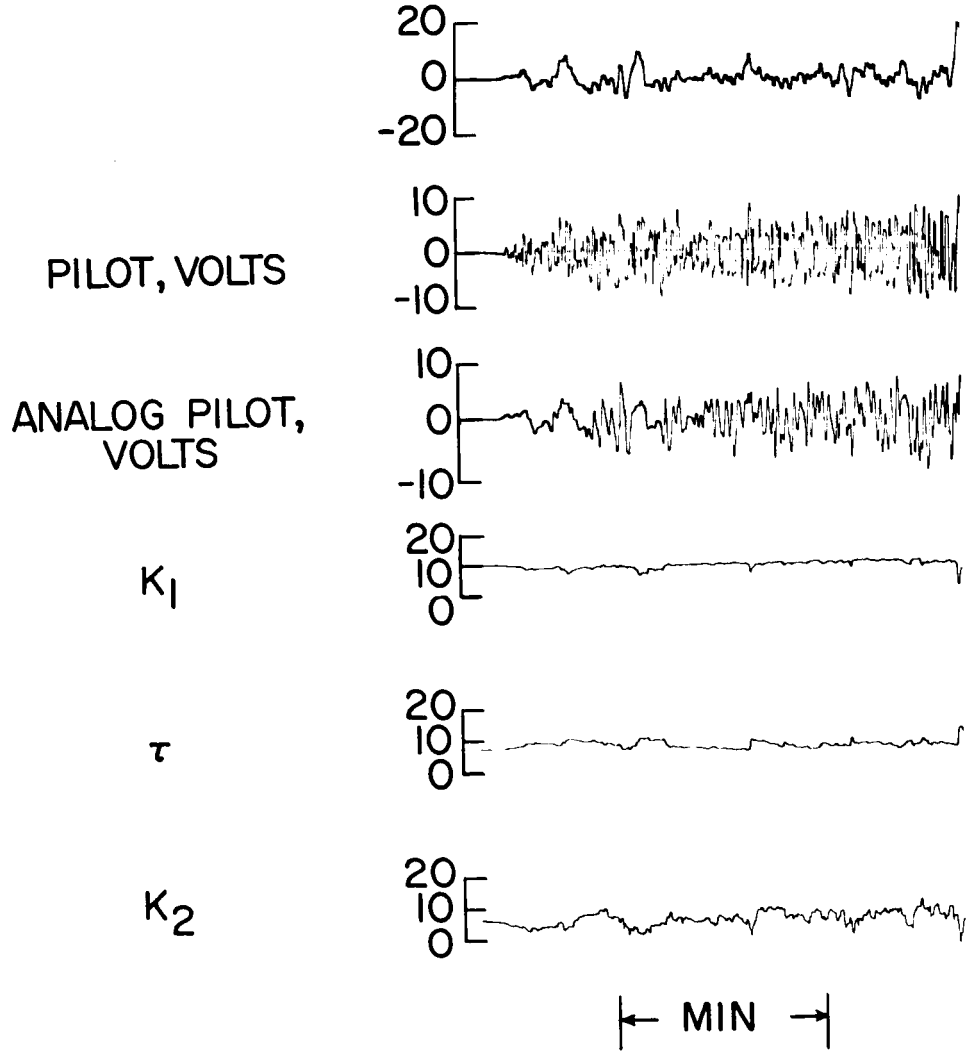

NASA

Figure 7.- Second axis of two without motion.

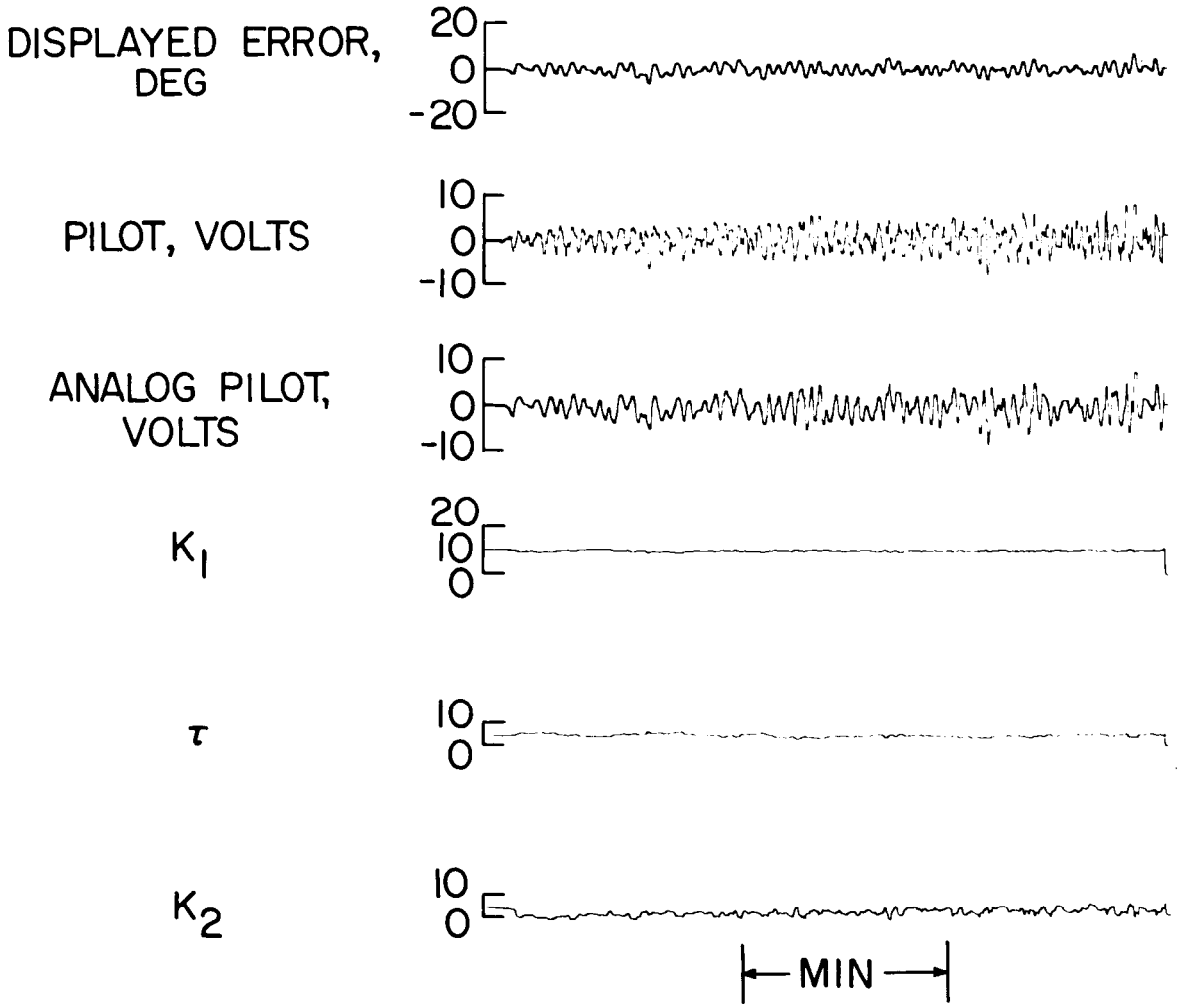

NASA

Figure 8.- Second axis of two with motion.

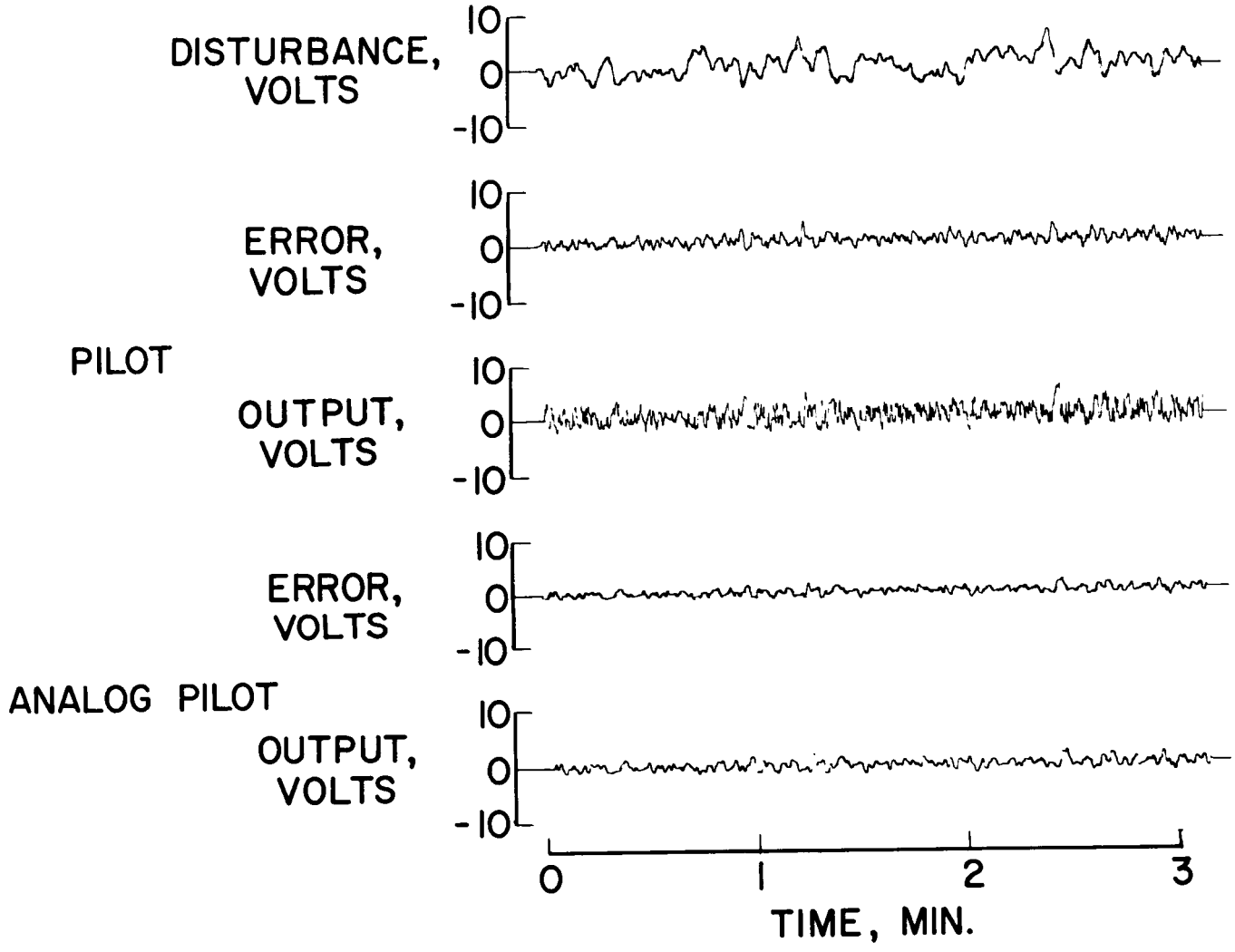

NASA

Figure 9.- Comparison of pilot in loop with analog pilot in loop for a dynamics of 2/s.

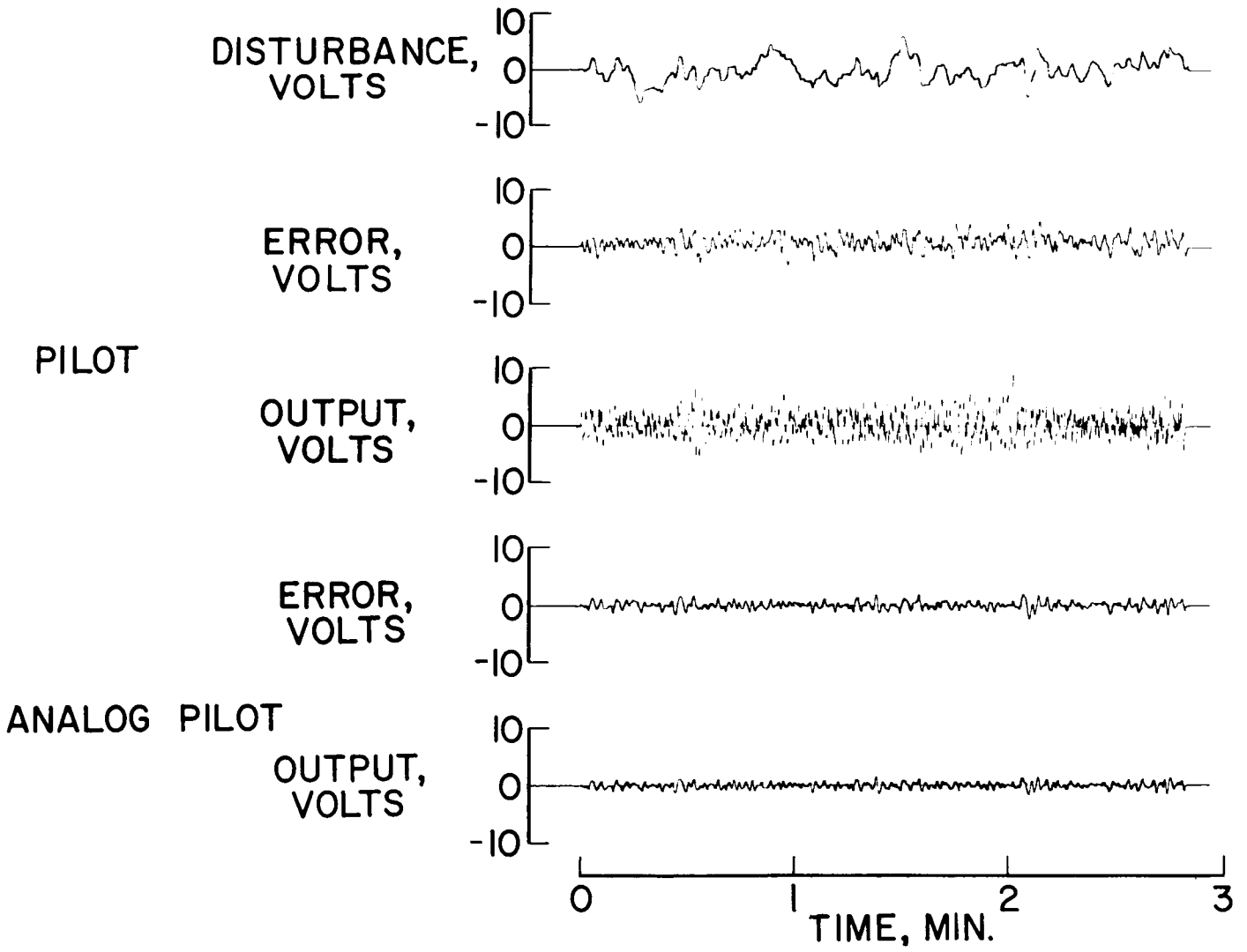

NASA

Figure 10.- Comparison of pilot in loop with analog pilot in loop for a dynamics of $\frac{10}{s(s+1)}$.

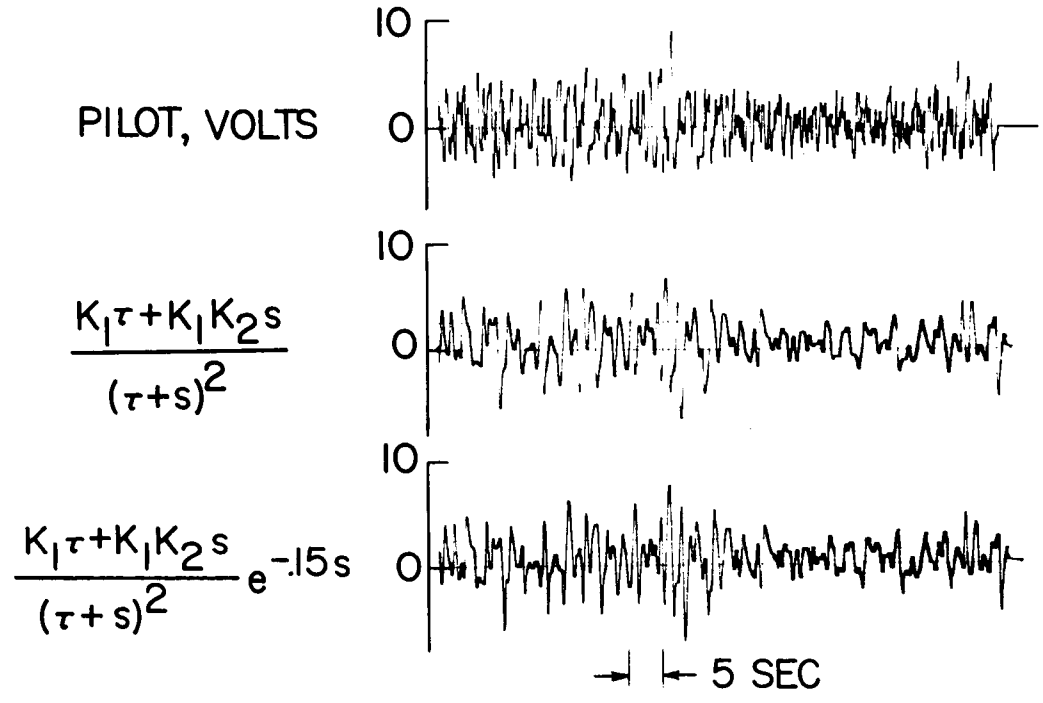

NASA

Figure 11.- Time histories illustrating match of different analog pilot forms to pilot with a dynamics of $\frac{10}{s(s+1)}$.

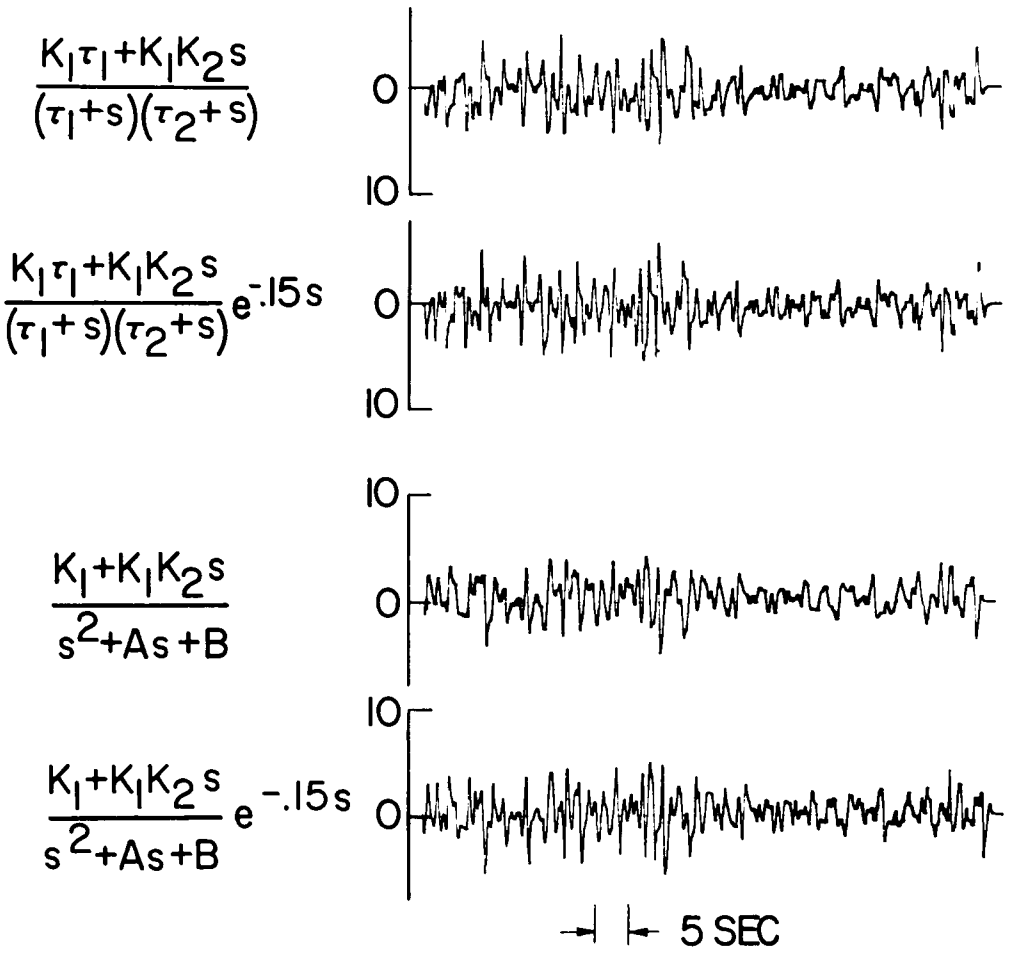

NASA

Figure 11.- Concluded.

NASA-Langley, 1963

MODEL FORM	MEASURED GAINS				CLOSED LOOP CHARACTERISTICS		
					OSCILLATORY		REAL ROOTS
	K_1	τ	τ_2	K_2	ω, RADIANS/SEC	ζ	
$\frac{K_1\tau + K_1K_2s}{(\tau + s)^2}$	2.5	6.5		5.5	3.45	0.37	-1.24, -10.1
$\frac{K_1\tau + K_1K_2s}{(\tau + s)^2} e^{-.15s}$	5	11		9			
	K_1	τ_1	τ_2	K_2			
$\frac{K_1\tau_1 + K_1K_2s}{(\tau_1 + s)(\tau_2 + s)}$	5	6	10	4	3.7	0.38	-1.7, -12.4
$\frac{K_1\tau_1 + K_1K_2s}{(\tau_1 + s)(\tau_2 + s)} e^{-.15s}$	7	16	17	10			
	K_1	K_2	A	B			
$\frac{K_1 + K_1K_2s}{s^2 + As + B}$	50	1	40	80	3.6	0.24	-1.0, -38.2
$\frac{K_1 + K_1K_2s}{s^2 + As + B} e^{-.15s}$	70	1	30	160			

NASA

Figure 12.- Summary of results with different model forms with a dynamics of $\frac{10}{s(s + 1)}$.